Design, Development, FEM analysis of Hybrid 12/14 BSRM with advanced controllers for Saispandan- Indian Total Artificial Heart for Destination Therapy (DT)

Pradeep Kumar Radhakrishnan*, Sujatha Mohanty**,Pulivarthi Nageshwar Rao*,Sivakrishna Rao G V*,Nagesh Kumar*,Bisoi A K** ,SivaPrasad*,Satyanarayana Murthy*, Satyanarayana M R S*,Ravishankar*,Srinivas*,Das P K***,Valluvan Jeevanandam****, Venugopal P**

Gitam University India*, AIIMS India **, IIT Kharagpur India***, University of Chicago USA ****

rpksai@hotmail.com, 9895270192

Abstract

12/14 Bearingless switched reluctance motor would be ideal according to our study for the Indian Total Artificial Heart- Saispandhan. Bearingless switched reluctance motor (BSRM) realizes both levitation and rotation by integrating both magnetic levitation and torque windings on the stator of the motor. It has a suspended rotor and decoupled control characteristics between speed and suspension force. The rotor has 14 poles and stator carries 12 poles. In 12 poles of the stator coordinately placed 4 poles are used for the suspension winding and diagonally placed 8 poles are used for the main winding motor. The rotor doesn't carry any winding. The bearingless concept is a plausible alternative to the magnetic bearing drives because as it provides numerous advantages like of friction-free, negligible thermal problems, lubrication free, less size ,minimal maintenance, low cost, compactness and no requirement of high power amplifiers. Levitation control of the rotor during starting, acceleration and deceleration of the rotor during rotation are the key phases besides stable levitation, in high-speed rotation of bearingless switched reluctance motor (BSRM).To realize the full potential of BSRM; it becomes necessary to overcome a few disadvantages associated with it. The BSRM requires a complex controller on account of its non-linear characteristics. Accurate shaft position information is essential to obtain high performance from the drive. To get smooth and acoustic noise less operation, the BSRM requires a good Torque ripple reduction control techniques.

Introduction:

The high-speed motors working in adverse environments involving high temperatures, radiation, and poisonous substances are often prone to motor breakdown. According to recent surveys, nearly 51% of motor breakdowns are only due to bearing failures which result in shut down of industrial process involving electric drives. The subsequent motor bearing failures may affect the modern industrial progress causing undesirable and unreliable conditions. Solving the motor bearing breakdown becomes the most challenging task for the researchers for a decade. Extensive research

has been going on developing bearing less technology by eliminating the conventional mechanical bearing system.

In case of high-speed and variable loading applications, the use of simple PI and Fuzzy control strategies alone is not effective in suspension controlling of the rotor and to keep less eccentric rotor displacements due to internal and external parameter variations. Hence, to get less rotor eccentric displacements and steady speed and torque profiles of the BSRM, new robust controllers like dynamic sliding mode controller (DSMC) and global sliding mode controller (GSMC) are proposed in this work.

The sliding mode control is a class of robust controllers. Sliding mode control (SMC) describes an optimal controller for a broad set of dynamic systems. The most distinguished feature of SMC is its ability to result in very robust control systems; in many of the cases invariant control systems results. Loosely speaking, the term 'invariant' means that the system is utterly insensitive to parametric uncertainty and external disturbances. It has reported widely, that SMC exhibits un-wanted motion so-called chattering, which produces due to discontinuity of the control action. However, the sliding mode control at high speeds has the disadvantages such as the chattering, increase of torque ripple and steady-state error due to its high switching gains. This specific performance makes the sliding mode control less attractive, even though it offers a stable and robust behavior.

In modern days, with the advent of power electronic devices and robust controllers and observers, the BSRM has gained importance. The advanced sliding mode controllers like GSMC and DSMC makes the system more stable and healthy. The problems encountered in reaching time and the chattering phenomenon which has obtained in the control scheme of SMC, a new global sliding mode control (GSMC) and dynamic sliding mode control (DSMC) schemes will reduce less extent. The proposed controllers have implemented because of BSRM's non-linearity and problems associated with it.

The theoretical exploration clarifies an operational principle and showed that the suggested motor could control translational motion, inclinational, and rotational movement individually.The proposed motor achieved a stable magnetically levitated rotation.

In addition, bearing less SRM fabricated into a prototype of the magnetically suspended rotor to investigate pump characteristics for a total artificial heart applications.

Simulation studies have conducted and analyzed the results under different testing conditions. From the results of suspension forces and rotor displacements in both X & Y-directions it is clearly understand that the results are robust, stable and the rotor is pulled back quickly to the center position due to the proposed controller's action.

The Features of the 12/14 BSRM Structure

Compared with the conventional bearingless SRM, main features of the 12/14 BSRM structure include:

Separated single winding: Only one winding is on each of the stator pole, which is relatively easier to manufacture compared with differential structure. Further, separated windings are on the separated torque and suspending force pole, which is different from general single-winding type. Moreover, the separated single winding is good for decoupling torque from radial force.

Wide suspending force region: Because pole arc of the suspending force is selected to be not less than one-rotor pole pitch, the overlap area between suspending force pole and rotor pole is constant at any rotor position. Therefore, compared with conventional bearing less SRM, available suspending force region is much wider.

Natural decoupling of torque from suspending force: Due to the constant overlapping area between suspending force pole and rotor pole, inductance variation of suspending force winding with respect to rotor position is very small with the fixed excitation current. Accordingly, the torque produced by the suspending force winding is very small. In other words, suspending force control has almost no influence on the torque control at arbitrary rotor position. Thus, torque control can be decoupled from suspending force control naturally.

Higher power density: 2/3 of the stator poles are used for the torque, so compared with 8/10 hybrid stator BLSRM, the power density is higher.

Low magnetic motive force (MMF): short flux paths are taken in the proposed structure, which will decrease the MMF.

Low core cost: in the proposed structure, there is no flux-reversal in the stator, which may reduce the core loss.

Operating Principle

The BSRM motor differs from the conventional motors in many respects and it consists of salient poles both in stator and rotor. The excitation is limited to stator only. The torque is developed by the tendency of the magnetic circuit to adopt a configuration of minimum reluctance. The excitation currents are unidirectional and discontinuous. The stator phases are sequentially excited to obtain continuous rotation. Besides, Due to the particularity of the structure of the proposed BSRM, there are two types of stator poles, i.e., suspending force pole and torque pole. Accordingly, the magnetic field distribution in the motor is complex; hence the design of controllers for BSRM is more complicated. Figure 1shows the structure and winding pattern of the motor.

The BSRM's stator consists of two types of salient poles. One is torque pole; the other is suspending force pole. There are two types of windings wound on the stator, one is suspension force winding to produce suspension force, and the other is torque winding to provide the reluctance torque. There are no windings on the rotor.

Two self-regulated DC supplies are given to the suspension and torque coils to achieve the de-coupled performance between net levitation force and motor torque. The suspension winding Coils Is1 and Is3 produce the radial force in Y-axis, and coils Is2 and Is4 produces the radial force in X-axis. The current in the Is2 stator pole generates positive x-direction suspending force, and the current in Is4 stator pole can make the negative x-direction suspending force. Similarly, the suspending forces for the y-direction can be generated by the currents which flow in suspending force poles Is1 and Is3 respectively. The stator main phase coils Ia and Ib produce a resultant rotational torque, and those called as phase-A and phase-B.

Hence, the BSRM drive needs a totally six hysteresis controllers to regulate both Suspension force and torque. Out of six, two are used as individual phase current controllers and remaining four suspension force current controllers are used to control the Suspension currents in both positive

and negative directions of X and Y-directions respectively. In the meanwhile, considering simplicity in control, two sets of asymmetric converters are applied in suspending force winding and torque winding, respectively. To get the constant suspending force, the suspending force pole arc is selected not to be less than one-rotor pole pitch. Therefore, the overlap area of the suspending force pole and the rotor pole is always the same.

Switching Control Strategy

The 12/14 bearingless SRM drive system only needs 12 power switches. As discussed in operating principle, the 12/14 BSRM is total a six phase drive. Therefore, eight power switches are required for controlling the four phase suspension windings and four power switches are required for two phase torque winding control. The detailed switch numbers are given in the table 1.1.

Operating Modes of the Asymmetric Converter

The asymmetric converters have widely applied in the SRM drives due to its advantages such as the capability of independent control of each phase and its four switching modes, Fig.2 shows were operating modes of the asymmetric converter. Mode 1 is magnetization mode in which positive dc-link voltage has applied to the winding; Mode 2 and 3 are free-wheeling modes in which the winding has short-circuited through an IGBT and a diode; mode 4 is demagnetization mode where the negative dc-link voltage has applied to the winding. In this demagnetization mode energy stored in the stator winding is returned to DC source.

Switching rules of hysteresis control method.

Based on the above suspending force current calculations, an asymmetric converter based on a hysteresis control method is applied to control the winding current. We can observe from Fig.3, the switching rules of the hysteresis control method. As shown in Fig. 2, for any rotor position, two currents in x-and y-directions are selected to input to the current controller, respectively. Meanwhile, which suspending force winding has conducted is determined by table 1.4. For instance, when the FX*>0 happens, the multi-switch will connect with the winding on the suspending force pole Is1, and then the winding on the suspending force pole Is1 is conducted consequently, according to current error, the switching state S of this winding can select as 1, 0 or -1, in which the switching state means the operating modes of the asymmetric converter. Therefore, the switching state 1 means magnetization mode; the switching state 0 means freewheeling mode; the switching state -1 means demagnetization mode. A detailed switching state rule of a hysteresis control method for proposed BSRM is as shown in table 1.2. FEM design details of BSRM

Bearing less Switched Reluctance Motors operation and resultant performances are characterized mainly by its flux-linkage characteristics. Unlike the other motors, these characteristics are nonlinear functions of stator current and rotor positions in BSRM. Therefore, the FEM is used for the analyzing the attributes of 12/14 BSRM structure, which includes magnetic flux distribution, inductance, torque and suspending force vs. position and current. The FEM design parameters of BSRM consist of 12 stator poles, 14 rotor poles. Among 12 stator poles, four suspension coils are placed coordinately on the stator to produce the suspending force in the X-Y direction to levitate the rotor in center position. The remaining eight diagonal poles are treated as torque poles to generate necessary torque. Entirely it is a six phase machine; all are individually excited with DC supply. The torque pole arc 12.85 degrees is taken exactly half to the suspension pole arc 25.71 degrees from the origin, to maintain the constant flux produced from the suspension poles.

Similarly, the number of turns in the torque coils has taken as 80, and the suspension coil turns are taken as 100 to maintain the strong magnetite field for levitation purpose. The air gap between the stator core and rotor core has taken as 0.3mm. Here is the list of some critical design parameters of 12/14 BSRM, shown in Table 1.3.

Modeling of Saispandan BSRM

Modeling of rotor for Suspension Control

The suspension control consists of X-directional and Y-directional displacement control of the rotor and the suspension forces in the X and Y-directions at standstill position are given below;

$$Fx=m\frac{d^2x}{dt^2}+kx \quad (1)$$

$$Fy=m\frac{d^2y}{dt^2}+ky+mg \quad (2)$$

Here, x_1, x_2, y_1, y_2 are taken as the state variables from equations (1) and (2), the equivalent-desired tracking rotor displacement equations are stated below;

$$\dot{x}_1=x_2 \quad \dot{y}_1=y_2$$

$$\dot{x}_2=-\frac{k_x}{m}x_1+\frac{F_x}{m}+F_{dx} \quad , \quad \dot{y}_2=-\frac{k_y}{m}y+\frac{F_y}{m}+F_{dy}+g \quad (3)$$

The electrical equivalent of the net suspending force produced in X-Y directions is given by;

$$\begin{bmatrix}F_x\\F_y\end{bmatrix}=\begin{bmatrix}K_{xxp} & K_{xyp} & K_{xxn} & K_{xyn}\\K_{yxp} & K_{yyp} & K_{yxn} & K_{yyn}\end{bmatrix}\begin{bmatrix}i_{xp}^2\\i_{yp}^2\\i_{xn}^2\\i_{xn}^2\end{bmatrix} \quad (4)$$

By equating the above two suspension force equations, we get

$$F_x=m\frac{d^2x}{dt^2}+kx=[K_X][I_x] \quad (5)$$

$$Fy=m\frac{d^2y}{dt^2}+ky+mg=[K_Y][I_Y] \quad (6)$$

Where, $K_X = \text{diag}[Kxxp \quad Kxyp \quad Kxxn \quad kxyn]$, $K_Y = \text{diag}[Kyxp \quad Kyyp \quad Kyxn \quad Kyyn]$ and

$$I_x = \begin{bmatrix} I_{xp}^{\,2} \\ I_{xn}^{\,2} \end{bmatrix}, \quad I_Y = \begin{bmatrix} I_{yp}^{\,2} \\ I_{yn}^{\,2} \end{bmatrix}$$

The equivalent desired tracking state space equations for rotor displacements are given by;

$$\begin{bmatrix} \dot{x}_1 \\ \dot{x}_2 \\ \dot{y}_1 \\ \dot{y}_2 \end{bmatrix} = \begin{bmatrix} 1 & 0 & 0 & 0 \\ -\frac{k}{m} & 0 & 0 & 0 \\ 0 & 0 & 1 & 0 \\ 0 & 0 & -\frac{k}{m} & -g \end{bmatrix} \begin{bmatrix} x_1 \\ x_2 \\ y_1 \\ y_2 \end{bmatrix} + \begin{bmatrix} 0 & 0 & 0 & 0 \\ Kxxp & Kxyp & Kxxn & Kxyn \\ 0 & 0 & 0 & 0 \\ Kyxp & Kyyp & Kyxn & Kyyn \end{bmatrix} \times \begin{bmatrix} i_{xp}^{\,2} \\ i_{yp}^{\,2} \\ i_{xn}^{\,2} \\ i_{xn}^{\,2} \end{bmatrix} \quad (7)$$

Modeling for The Speed control of BSRM

The Vector of flux linkages 'Ψ', the vector of Voltages 'V', phase current vector 'i', the vector of the mutual inductance matrix 'N' and phase resistances 'r' are defined for the motor dynamics are given below;

$$\frac{d\psi}{dt} = -rN(\theta)\psi + V + w_\psi \quad (8)$$

$$\frac{dw}{dt} = \frac{T_e - T_l}{J} - \frac{B}{J}w + \frac{T_e}{J} + w_w \quad (9)$$

$$\frac{d\theta}{dt} = w + w_\theta \quad (9)$$

$$i = N(\theta)\psi \quad (10)$$

Results and discussions:

FEM Analysis:

To get better and accurate motor performance characteristics, a FEM model 12/14 BSRM was designed and analyzed. At different winding currents, the main torque winding inductance and main torque values w.r.t rotor position are taken and presented. These numerical data of FEM design 12/14 BSRM will support in control of the motor.

Fig.3 shows the flux distribution of BSRM when only all suspension windings are excited. Fig.4 (a) & (b) shows the short flux paths without flux reversal in the stator core, which decrease the core losses, as well as MMF requirement and the flux linkage values, reaches its maximum value when the rotor teeth begin to overlap with the stator teeth. The inductances of the main windings

and suspension windings are taken at different values of control currents when the rotor is at geometric Centre. The inductance of main torque winding varies with rotor positions as shown in Fig.5. The overlap region among stator torque poles and rotor poles is the function of the rotor position, due to which inductance of the main torque winding varies with rotor positions.Fig.6 illustrates the inductance profiles of the suspending winding w.r.t rotor position, and it has observed that the suspension winding inductance does not change with rotor position. The pole arc of the levitation force pole is more prominent than one rotor pole pitch. Hence the suspension winding inductance value is almost constant. From the Fig.5 and Fig.6, it can be inferred that with the increase of both winding currents, the maximum amount of inductances of both types of windings are decreasing due to the stator core saturation effect. When both the windings are conducted together the saturation effect is negligible.

The nonlinear torque profiles of BSRM w.r.t rotor position where the torque is directly proportional to the square of phase currents and the rate of change of phase inductance with respect to the rotor positions. With the similarity of all torque poles, here we considered the torque pole of Phase-A, to observe the torque profile at different currents with respect to rotor position. From the Fig.7, it has found that the torque values gradually increase up to 7-degrees and decreases to a minimum amount of 0.2(N-mt) nearly 13 degrees. From the above numerical FEM analysis it can be concluded that, when the edge of the rotor teeth pole coincides with the stator teeth pole at all angles of the rotor, the torque produced from both the phases will be maximum. The non-linear characteristics of static torque increase with the increase in current.

From the Fig.8 & 9, it can be observed that net suspending forces produced by suspending force windings Is1 & Is2 are increases proportional to the suspension currents. From the above figures, it can found that there is a little influence on the suspension force at different torque currents. Therefore, the 12/14 BSRM structure is simple to control, and it has independent control between suspension force and torque.

The net suspending force is changed a little with the rotor position in Y-direction. The X-direction net suspension force shows a significant variation with respect to the rotor positions.

The magnitude of the radial (suspension) force is proportional to suspension control current, as the value of the current increases the radial force also increases, which has observed in Fig.10, at different values of control currents of coil 1&3. The suspension force for a negative value of currents is the same as the positive values of currents (mirror image), which shows that radial force is independent of the polarity of the current.

Conclusions

Excellent decoupling environment between stator torque control and suspension force control is found at different values of currents[41-44]. Suspension force and motor torque increases with increase of rotor eccentric displacements in the Y direction. In addition to the improved performance characteristics GSMC cancels the reaching mode, reduces chatting and overcomes the disturbance and time delay[45-48]. The closed loop operation of BSRM system with conventional and global sliding mode controllers were found to be working very well under different loading conditions[48-58].GSMC based SMO offers less chattering greater stability and accurate rotor displacement, position and speeds under unexpected changes of reference and loading conditions. We are now making a miniature version of this motor for Saispandan Total Artificial Heart - The Gitam Heart.

Table 1.1 Requirement of Switch numbers for 12/14 BSRM

12/14 BSRM	Number of power switches	Total
Torque winding (two phase)	2 per phase	4
Suspending force winding (four phase/four pole)	2 per pole	8

Table 1.2 Switching state rule of hysteresis control method for BSRM.

Desired force	Suspending force poles selection	Enable-Is1	Enable-Is2	Enable-Is3	Enable-Is4
If $F_x \geq 0, F_y \geq o$	Is1 & Is2	1	1	0	0
If $F_x \geq 0, F_y \leq o$	Is2 & Is3	0	1	1	0
If $F_x \leq 0, F_y \leq o$	Is3 & Is4	0	0	1	1
If $F_x \leq 0, F_y \geq o$	Is4 & Is1	1	0	0	1

Table 1.3 Design parameters of 12/14 BSRM

S.no	Design Parameters of BSRM	Dimensions
1	Outer diameter of stator (mm)	56mm
2	Stator yoke thickness(mm)	3.85mm
3	Stator inner diameter. (mm)	30.1 mm
4	Axial stack length (mm)	20mm
5	suspension pole arc(deg)	25.71 deg
6	The torque pole arc(deg)	12.85deg
7	Rotor pole arc (deg)	12.85deg
8	Rotor yoke thickness (mm)	4.85mm

Fig.1 12/14 BSRM Structure and Winding pattern

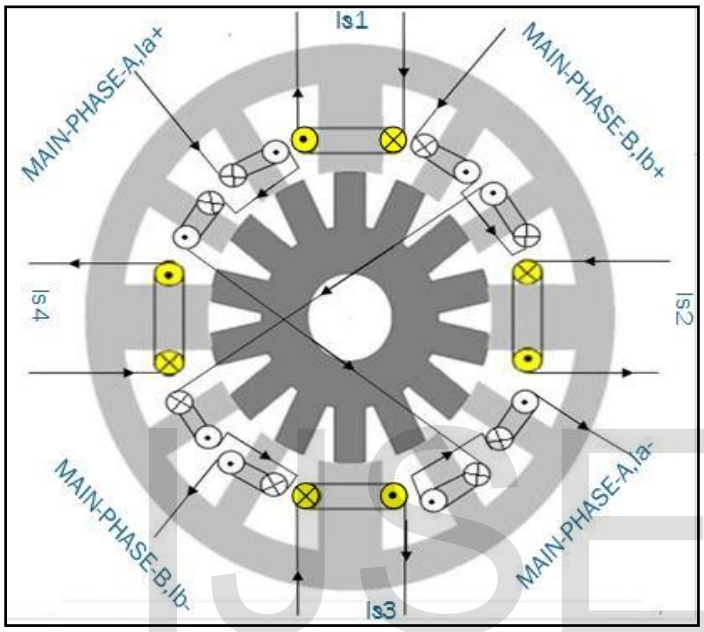

Figure 2 Operating Modes of the Asymmetric Converter

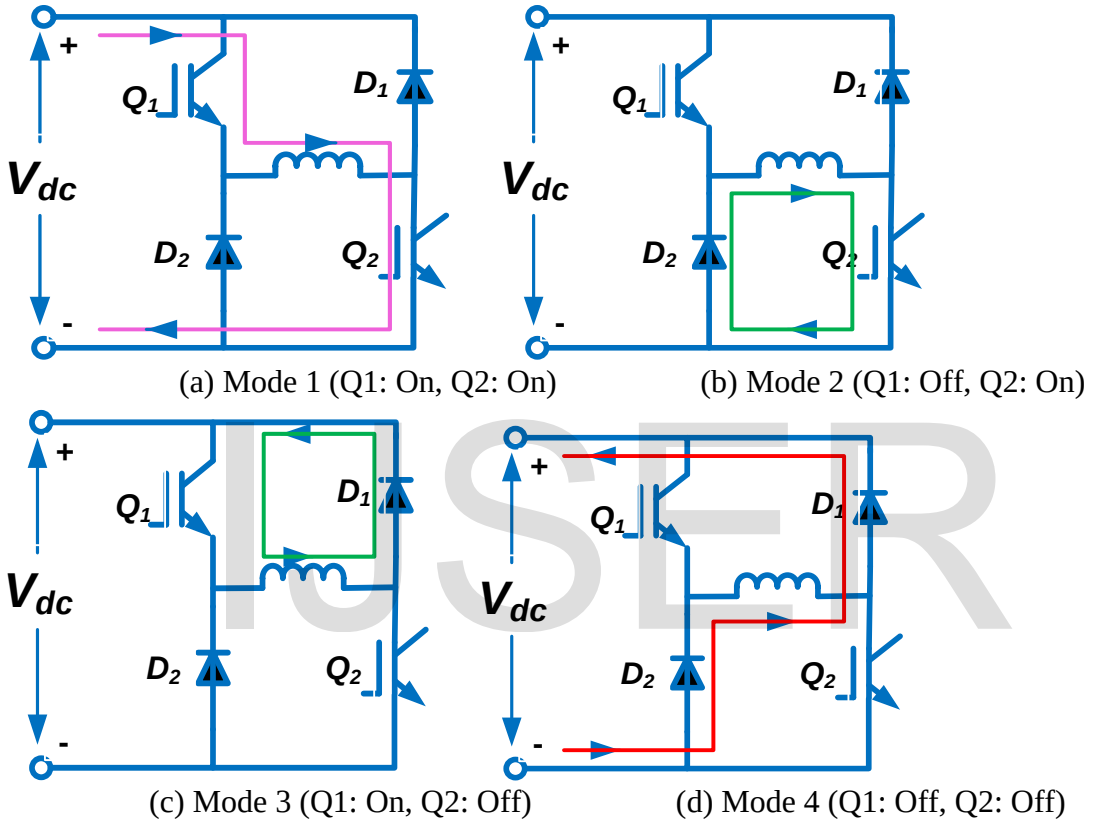

(a) Mode 1 (Q1: On, Q2: On) (b) Mode 2 (Q1: Off, Q2: On)

(c) Mode 3 (Q1: On, Q2: Off) (d) Mode 4 (Q1: Off, Q2: Off)

Figure 3 Switching rules of hysteresis control method

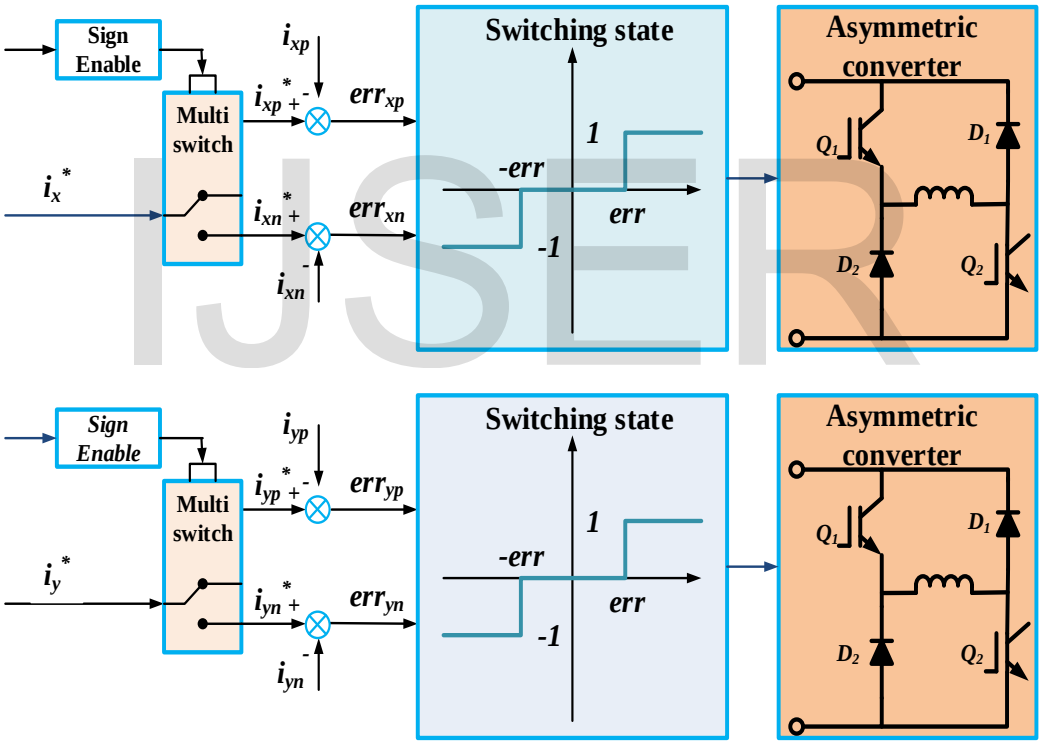

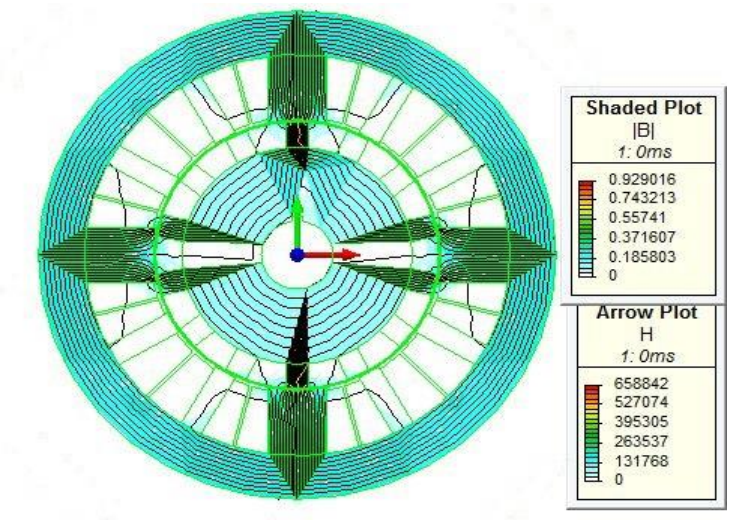

Fig. 3 Flux distribution of all suspension Windings.

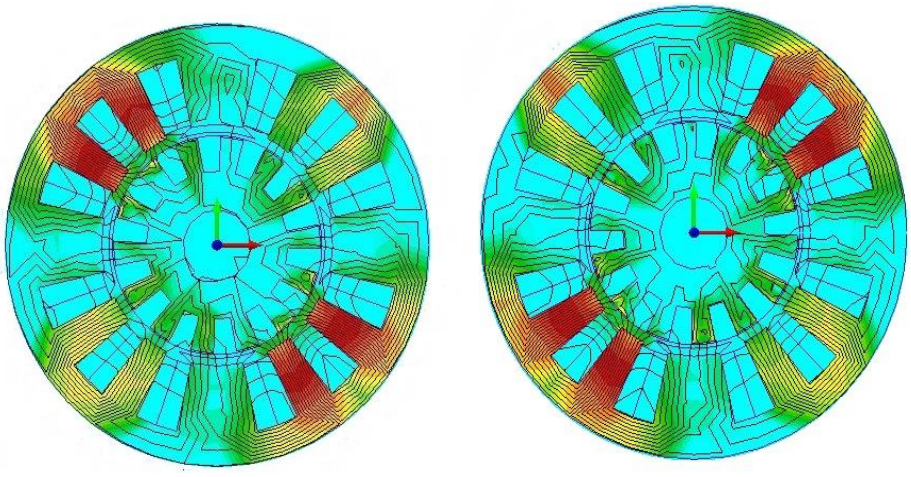

Fig. 4(a) Fig. 4(b).

Main winding short flux distributions of Phase-A & Phase-B.

Figure 5 Main winding inductance of the main torque winding varies with rotor positions.

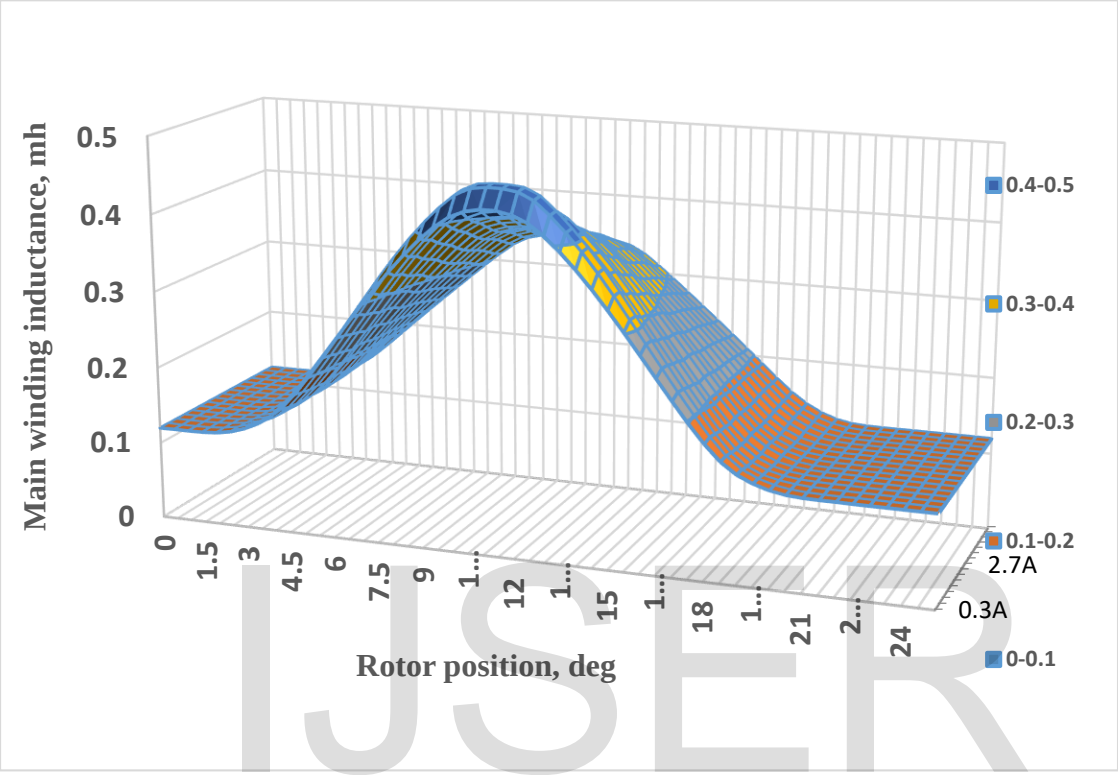

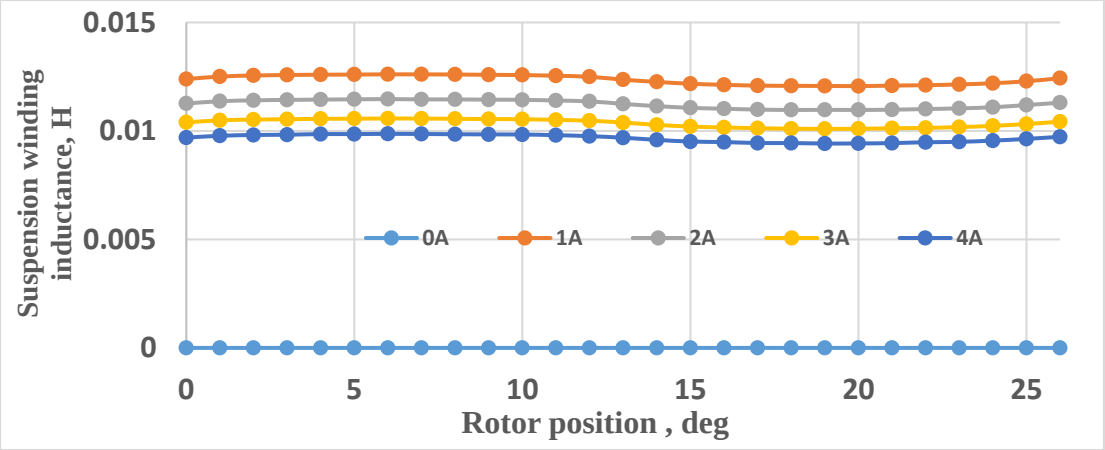

Figure 6 Suspension winding inductances at different suspension currents.

Figure 7. Non linear torque profile of main winding.

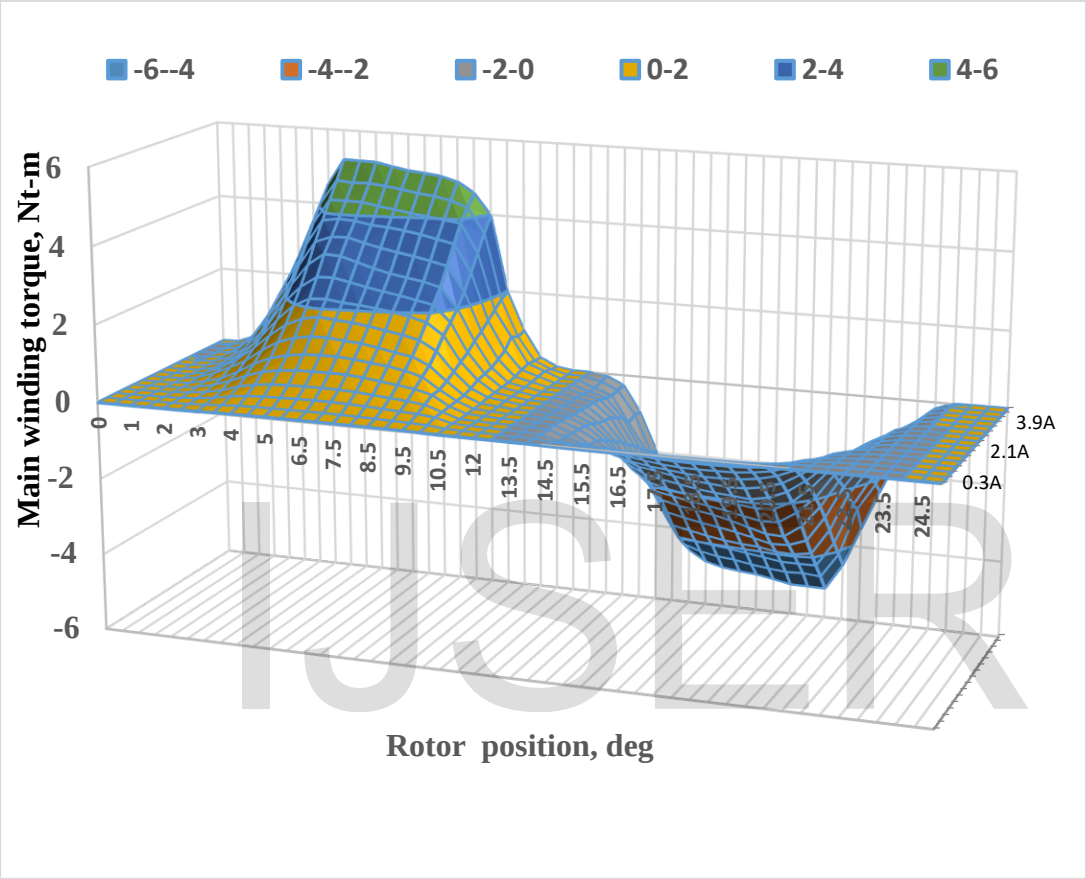

Figure 8 Net force values of suspension coil-Is1

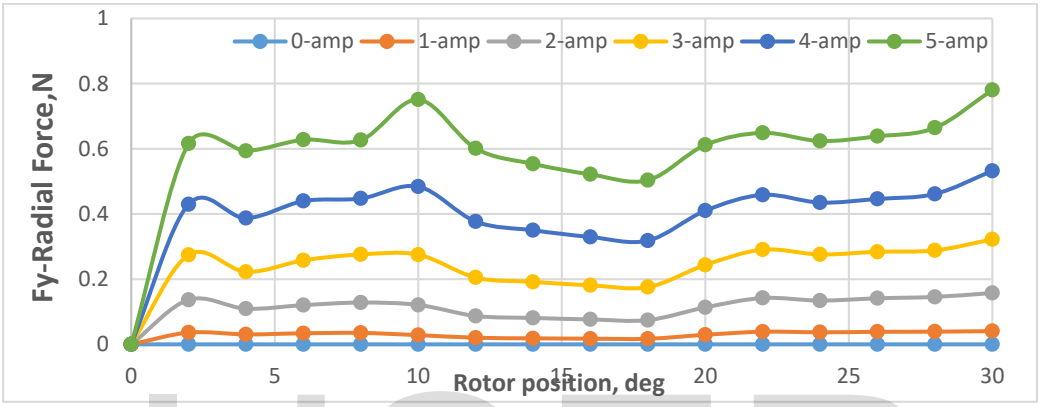

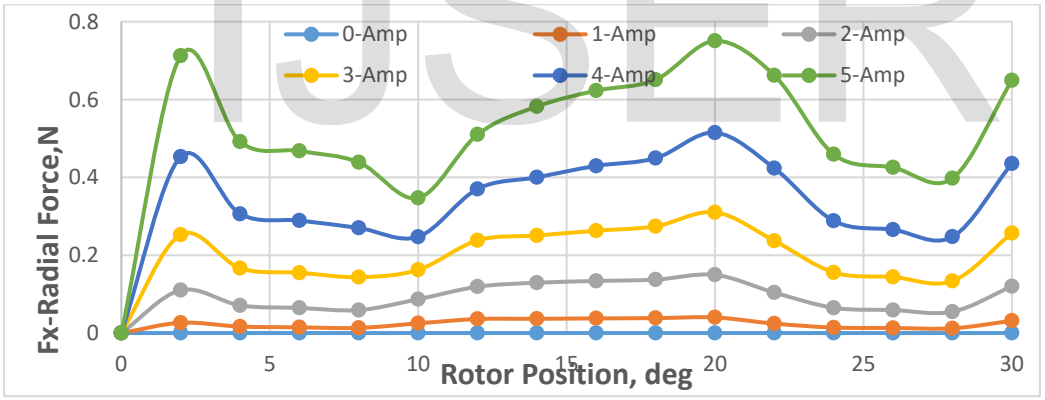

Fig.9 Net force values of suspension coil- Is2.

Fig.10 Radial Force versus Control Current.

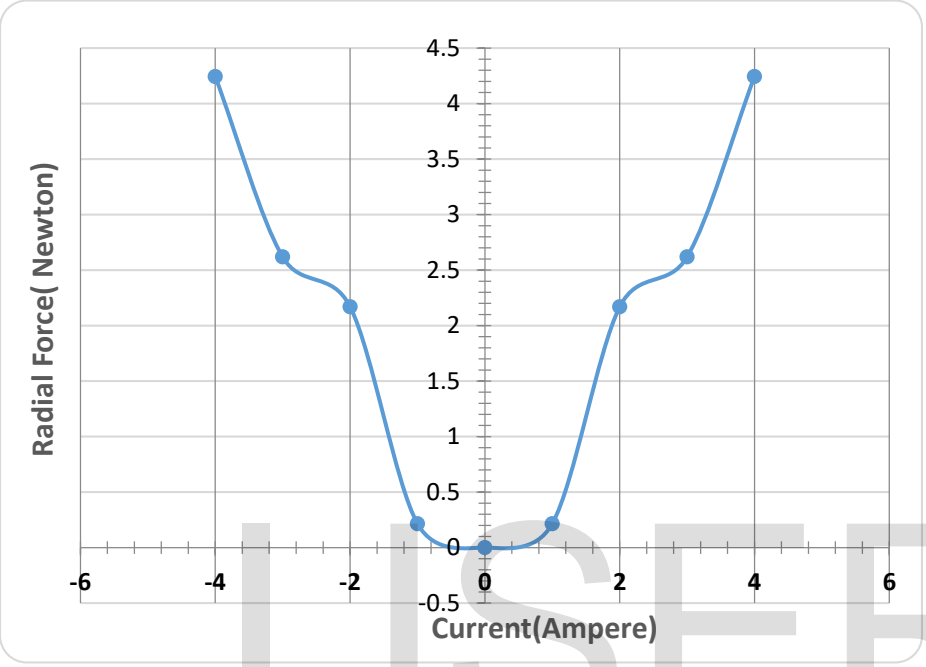

REFERENCES

1.M. Takemoto, A. Chiba and T. Fukao, A New Control Method of Bearingless Switched Reluctance Motors Using Square-wave Currents, Proceedings of the IEEE Power Engineering Society, Singapore, 2000, 375-380.

2.M. Takemoto, H. Suzuki & A. Chiba, Improved Analysis of a Bearing less Switched Reluctance Motor, IEEE Transactions 0n Industrial Applications, 37(1) (2001) 26-34.

3.L. Chen and W. Hofman, Analytically Computing Winding Currents to Generate Torque and Levitation Force of a New Bearingless Switched Reluctance Motor, in Proceedings of 12th International Power Electronics and Motion Control Conference, Portoroz Slovenia, 2006: 1058-1063.

4.H. J. Wang, D. H. Lee & J. W. Ahn, Novel Bearing less Switched Reluctance Motor with Hybrid Stator Poles: Concept, Analysis, Design and Experimental Verification, International Conference On Electrical. Machines and Systems, 2008, 3358-3363.

5.Dong-Hee Lee &Jin-Woo Ahn, Design and Analysis of Hybrid Stator Bearing less SRM, Journal of Electrical Engineering& Technology, 6(1), 2011, 94-103.

6.H. Wang, Y. Wang, X. Liu and J. W. Ahn, Design of novel bearingless switched reluctance motor, in IET Electric Power Applications, vol. 6, no. 2, pp. 73-81, February 2012.

7.Dong-Hee Lee, Jin-Woo Ahn, Design and Analysis of Hybrid Stator Bearingless SRM, Journal of Electrical Engineering & Technology, 2011, 6(1): 94-103

8.Hyeung-Sik Choi, Yong-Heon Park, Yongsung Cho and Minho Lee, Global sliding-mode control. Improved design for a brushless DC motor, in IEEE Control Systems, vol. 21, no. 3, pp. 27-35, June 2001.

9.Z. Cheng, C. Hou and X. Wu, Global Sliding Mode Control for Brushless DC Motors by Neural Networks, 2009 International Conference on Artificial Intelligence and Computational Intelligence, Shanghai, 2009, pp. 3-6

10.Leipo Liu · Zhengzhi Han ·Wenlin Li, Global sliding mode control and application in chaotic systems, Springer, Nonlinear Dynamics-2009, 56: 193–198.

11.Roy A.McCann, Mohammad S.Islam& Iqbal Hussain,"Application of a sliding mode observer for Position and Speed Estimation in Switched Reluctance Motor drive", IEEE Transactions on Industry Applications, 37 (2001) 51-58.

12.Y.J.Zhan, C.C.Chan&K.T.Chau, "A novel sliding-mode observer for Indirect sensing of Switched reluctance Motor drives", IEEE Transactions on Industrial Applications, 46 (1999) 390-397.

13.Mohammad.S.Islam, Iqbal Hussain, and RobertJ.Veillette&CelalBatur,"Design and performance analysis of sliding mode observers for sensor less operation of switched reluctance motors",IEEE Transactions on Industrial. Applications, 3, (2003) 383-389.

14.Hosham Salim, Abduljabbar O. H.Alshammery,"A Practical Drive System with Accurate Rotor Position Detection for a Switched Reluctance Motor, Arabian Journal for Science and Engineering, 2013, 38:2765–2772.

15.Koshkouei, A.J. & Burnham, Keith &Zinober, Alan, Dynamic Sliding Mode Control Design'. Control Theory and Applications, IEE Proceedings -. 152. 392 - 396. 10.1049/ip-cta: 20055133.

16 Gholipour, Sara &Shandiz, Heydar, Dynamic Sliding Mode Control based on Fractional calculus subject to uncertain delay based chaotic pneumatic robot, 2013.

17Inanc, Nihat&Ozbulur, Veysel, Torque ripple minimization of a switched reluctance motor by using continuous sliding mode control technique. Electric Power Systems Research. 66. 241-251. 2003.

18.Falahi, M &Salmasi, F.R., A sliding mode controller for switched- reluctance motor with iterative learning compensation. 631-635.2007.

19.Ro, Hak-Seung&Jeong, Hae-Gwang& Lee, Kyo-Beum., Torque ripple minimization of switched reluctance motor using direct torque control based on sliding mode control. IEEE International Symposium on Industrial Electronics. 1-6. 2013.

20.Zan, Xiaoshu. Switched reluctance motor speed performance simulation study based on torque ripple suppression. 253-257, 2013.

21.N. Kurita, T. Ishikawa, N. Saito, T. Masuzawa, and D. Timms, "A doublesided stator type axial self-bearing motor development for total artificial heart," in Proc. IEEE Int. Elect. Mach. Drives Conf., Miami, FL, USA, 2017, Paper TO243.

22.American Heart Association, "Heart disease and stroke statistics—2009 update," Amer. Heart Assoc. Statist. Committee Stroke Statist. Subcommittee, Dallas, TX, USA, in CIRCULATION, vol. 119, no. 3, pp. e21–e181, 2009.

23.P. A. Watterson, J. C. Woodard, V. S. Ramsden, and J. A. Reizes, "Ventr assist hydrodynamically suspended, open, centrifugal blood pump," J. Artif. Organs, vol. 24, no. 6, pp. 475–477, 2001

24.T. Masuzawa, S. Ezoe, T. Kato, and Y. Okada, "Magnetically suspended centrifugal blood pump with an axially levitated motor," J. Artif. Organs, vol. 27, no. 7, pp. 631–638, 2003.

24.H. Hoshi, T. Shinshi, and S. Takatani, "Third-generation blood pumps with mechanical noncontact magnetic bearings," J. Artif. Organs, vol. 24, no. 6, pp. 324–338, 2006.

25.H. Fumoto et al., "In vivo acute performance of the cleveland clinic self-regulating, continuous-flow total artificial heart," J. Heart Lung Transplantation, vol. 29, no. 1, pp. 21–26, 2010.

26.O. H. Frazier and W. E. Cohn, "Continuous-flow total heart replacement device -implanted in a 55-year-old man with end-stage heart failure and severe amyloidosis," TexasHeart Inst. J., vol. 39, no. 4, pp. 542–546, 2012.

27.N. Kurita, D. Timms, N. Greatrex, and T. Masuzawa, "Axial magnetic bearing development for the BiVACOR rotary BiVAD/TAH," in Proc. 11th Int. Symp. Magn. Bearing, Nara, Japan, 2008, pp. 217–224.

28.N. A. Greatrex, D. L. Timms, N. Kurita, E. W. Palmer, and T. Masuzawa, "Axial magnetic bearing development for the BiVACOR rotary BiVAD/TAH," IEEE Trans. Biomed. Eng., vol. 57, no. 3, pp. 714–721,Mar. 2010.

29.N. Kurita, D. Timms, N. Greatrex, M. Kleinheyer, and T. Masuzawa, "Optimization design of magnetically suspended system for the BiVACOR total artificial heart," in Proc. 14th Int. Symp. Magn. Bearing, Linz, Austria, 2014, pp. 437–440.

30.N. Kurita, T. Ishikawa, H. Takada, and T. Masuzawa, "Design and simulation of a double stator type axial magnetically levitated motor," in Proc. COMPUMAG, Budapest, Hungary, 2013, Paper PC6-17.

31.N. Kurita and T. Ishikawa, "A study on a double stator type axial magnetically levitated motor," in Proc. IEEE Int. Symp. Ind. Electron.,Taipei, Taiwan, 2013, Paper 5177.

32.K. Shimbo, I. Tomita, O. Ichikawa, C. Michioka, A. Chiba, and T.Fukao, "Axial gap length and the maximum torque of shaftless axial gapbearingless motors," (in Japanese), in Proc. IEEJ Annu. Meeting, 1997,Paper 1218.

33.K. Chongkwanyuen, O. Ichikawa, C. Michioka, A. Chiba, and T. Fukao,"Inclination control of axial gap bearingless motors," (in Japanese), inProc. IEEJ Annu. Meeting, 1997, Paper 1219.

34.N. Kurita, T. Ishikawa, H. Takada, and G. Suzuki, "Proposal of apermanent magnet hybrid-type axial magnetically levitated motor," IEEJJ. Ind. Appl., vol. 4, no. 4, pp. 339–345, 2015.

35.S. Ueno, T. Fukuura, and T. V. Toan, "A 5-DoF active controlled disk typepm motor with cylindrical flux paths," in Proc. 14th Int. Symp. Magn.Bearings, Linz, Austria, 2014, pp. 216–219.

36.N. Kurita, T. Ishikawa, H. Takada, and T. Masuzawa, "Development ofthe left ventricular assist device by use of the double side stator type axialmagnetically levitated motor," in Proc. Int. Soc. Rotary Blood Pumps,Yokohama, Japan, 2013, Paper P-4.

37.N. Kurita, T. Ishikawa, N. Saito, and T. Masuzawa, "A double side statortype axial self-bearing motor development for the left ventricular assistdevices," Int. J. Appl. Electromagn. Mech., vol. 52, pp. 199–206, 2016.

38.G. Schweitzer et al., Magnetic Bearings: Theory, Design, and Applicationto Rotating Machinery. Berlin, Germany: Springer, 2010.

39.Sun, X., Y. Chen, S. Wang, G. Lei, Z. Yang, and S. Han, "Core losses analysis of a novel 16/10 segmented rotor switched reluctance BSG motor for HEVs using nonlinear lumped

parameter equivalent circuit model," IEEE/ASME Trans. Mech., Vol. 23, No. 2, 747–757, Feb. 2018.

40.Xue, X. D., K. W. E. Cheng, T. W. Ng, and N. C. Cheung, "Multi-objective optimization design of in-wheel switched reluctance motors in electric vehicles," IEEE Trans. Ind. Electron., Vol. 57, No. 9, 2980–2987, Sep. 2010.

41.Torkaman, H., E. Afjei, and M. S. Toulabi, "New double-layer-per-phase isolated switched reluctance motor: Concept, numerical analysis, and experimental confirmation," IEEE Trans. Ind. Electron., Vol. 59, No. 2, 830–838, Feb. 2012

42.Sun, X., L. Chen, H. Jiang, Z. Yang, J. Chen, and W. Zhang, "High-performance control for a bearingless permanent-magnet synchronous motor using neural network inverse scheme plus internal model controllers," IEEE Trans. Ind. Electron., Vol. 63, No. 6, 3479–3488, Jun. 2016.

43.Asama, J., Y. Hamasaki, T. Oiwa, and A. Chiba, "Proposal and analysis of a novel single-drive bearingless motor," IEEE Trans. Ind. Electron., Vol. 60, No. 1, 129–138, Jan. 2013

44.Sun, X., Z. Shi, L. Chen, and Z. Yang, "Internal model control for a bearingless permanent magnet synchronous motor based on inverse system method" IEEE Trans. Energy Convers., Vol. 31, No. 4, 1539–1548, Dec. 2016

45.Matsuzaki, T., M. Takemoto, S. Ogasawara, S. Ota, K. Oi, and D. Matsuhashi, "Operational characteristics of an IPM-type bearingless motor with 2-pole motor windings and 4-pole suspension windings," IEEE Trans. Ind. Appl., Vol. 53, No. 6, 5383–5392, Nov.–Dec. 2017.

46.Sun, X., L. Chen, and Z. Yang, "Overview of bearingless permanent-magnet synchronous motors," IEEE Trans. Ind. Electron., Vol. 60, No. 12, 5528–5538, Dec. 2013.

47.Sun, X., L. Chen, Z. Yang, and H. Zhu, "Speed-sensorless vector control of a bearingless induction motor with artificial neural network inverse speed observer," IEEE/ASME Trans. Mech., Vol. 18, No. 4, 1357–1366, Aug. 2013

48.Cao, X., J. Zhou, C. Liu, and Z. Deng, "Advanced control method for single-winding bearingless switched reluctance motor to reduce torque ripple and radial displacement," IEEE Trans. Energy Convers., Vol. 32, No. 4, 1533–1543, Dec. 2017.

49.Wang, H., J. Bao, B. Xue, and J. Liu, "Control of suspending force in novel permanent-magnetbiased bearingless switched reluctance motor," IEEE Trans. Ind. Electron., Vol. 62, No. 7, 4298– 4306, Jul. 2015.

50.Cao, X., Z. Deng, G. Yang, and X. Wang, "Independent control of average torque and radial force in bearingless switched-reluctance motors with hybrid excitations," IEEE Trans. Power Electron., Vol. 24, No. 5, 1376–1385, Jul. 2009.

51.Liu, J., H. Wang, J. Bao, G. Zhou, and F. Zhang, "A novel permanent magnet biased bearingless switched reluctance motor," IEEE Trans. Ind. Electron., Vol. 61, No. 12, 4342–4347, Sep. 2013.

52.Wang, H., J. Liu, J. Bao, and B. Xue, "A Novel bearingless switched reluctance motor with a biased permanent magnet," IEEE Trans. Ind. Electron., Vol. 61, No. 12, 6947–6955, Dec. 2014. Progress In Electromagnetics Research C, Vol. 89, 2019 205

53.Xue, B,. H. Wang, and J. Bao, "Design of novel 12/14 bearingless permanent biased switched reluctance motor," IEEE International Conference on Electrical Machines and Systems., 2655– 2660, Oct. 2014.

54.Wei, P., D. Lee, and J. Ahn, "Design and analysis of double stator type bearingless switched reluctance motor," Transactions of the Korean Institute of Electrical Engineers, Vol. 60, No. 4, 746–752, 2011.

55.Zhang, J., H. Wang, L. Chen, C. Tan, and Y. Wang, "Multi-objective optimal design of bearingless switched reluctance motor based on multi-objective genetic particle swarm optimizer," IEEE Trans. Magn., Vol. 54, No. 1, 113, Oct. 2017.

56. Chen, L. and W. Hofmann, "Speed regulation technique of one bearingless 8/6 switched reluctance motor with simpler single winding structure," IEEE Trans. Ind. Electron., Vol. 59, No. 6, 2592– 2600, Jun. 2012.

57.Cao, X. and Z. Deng, "A full-period generating mode for bearingless switched reluctance generators," IEEE Transactions on Applied Superconductivity, Vol. 20, No. 3, 1072–1076, Mar. 2010.

58.Liu, J., X. Zhang, H. Wang, and J. Bao, "Iron loss characteristic for the novel bearingless switched reluctance motor," IEEE, 586–592, Oct. 2013

.